Lifetime instabilities in gallium doped monocrystalline PERC silicon solar cells

Nicholas E. Grant [a],[**], Jennifer R. Scowcroft [a], Alex I. Pointon [a], Mohammad Al-Amin [b], Pietro P. Altermatt [c], John D. Murphy [a],[*]

[a] School of Engineering, University of Warwick, Coventry, CV4 7AL, UK
[b] WMG, University of Warwick, Coventry, CV4 7AL, UK
[c] Trina Solar Limited, Changzhou, 213031, China

ARTICLE INFO

ABSTRACT

Gallium doped silicon is an industrially viable alternative to boron doped silicon for photovoltaics, and is assumed to be immune from light-induced degradation. We have studied light soaking for >1000 h of industrially fabricated passivated emitter and rear cell (PERC) devices formed from monocrystalline gallium and boron doped substrates, with cell properties monitored using a non-contact photoluminescence imaging proxy method. As-fabricated stabilised boron doped cells did not degrade or underwent a slight improvement, whereas as-fabricated gallium doped cells which had not been intentionally stabilised experienced a slight (~5%) deterioration which then recovered. When PERC devices were subjected to a 200–300 °C dark anneal before light soaking, significant differences in the cell degradation signatures were observed. Degradation characteristic of light and elevated temperature induced degradation (LeTID) was observed for boron and gallium PERC solar cells, with the onset of degradation taking longer, and the severity being less, with gallium. Investigation of stripped gallium PERC devices with room temperature surface passivation revealed bulk lifetime degradation correlates with the cell-level degradation. When the cells were stripped and passivated with aluminium oxide, a complete change in the degradation behaviour was observed, with no degradation occurring in the gallium case and boron-oxygen-like degradation observed for boron. This indicates that dielectric passivation is not suitable for lifetime degradation diagnosis in stripped cells. Gallium retains advantages over boron doping with stabilisation processes not generally required, but manufacturers need to be aware of possible low-temperature lifetime instabilities when developing future fabrication processes, such as for passivated contact structures.

1. Introduction

The majority of today's solar cells are made from *p*-type silicon wafers with boron as the electrically active dopant. The excess charge carrier lifetime (henceforth just "lifetime") in silicon can reduce under illumination leading to reduced solar cell efficiencies, and this light-induced degradation (LID) can occur in several ways. An important form of LID occurs in boron doped silicon, in which recombination centres form in a way related to the boron and grown-in oxygen levels. This degradation mechanism has been studied for almost 50 years [1] and the large body of literature in this area has been recently reviewed [2,3]. Another effect occurs in thermally processed (including fired) wafers and is referred to as light and elevated temperature induced degradation (LeTID). LeTID has been observed in multicrystalline silicon (mc-Si) [4–6], float-zone silicon (FZ-Si) [7,8] and Czochralski silicon [9, 10]. It involves an initial lifetime degradation but typically recovers over time, with degradation and recovery rates depending on thermal history. The physical origin of LeTID is unclear, but similarities across the range of material types suggest a common mechanism [11]. Other forms of LID occur in silicon which is contaminated with metals, such as copper [12].

Workarounds for boron-oxygen related LID exist [13]. Today's commercial boron doped silicon solar cells are exposed to a so-called re-generation process by annealing them at the end of their fabrication with high temperature either combined with high illumination intensity or high current density in the dark. From the experience of the

---

industrial co-author of this paper, the majority of large manufacturers in China apply the second annealing method and often warrant a degradation rate smaller than 0.5%$_{relative}$ per year over 30 years in their modules. This means that an initially 20% efficient PERC module degrades to not lower than 17%$_{absolute}$ efficiency in 30 years. After the warranty runs out and the module is depreciated, many modules are expected to deliver power for another 10–20 years with one other replacement of inverters, which makes the after-warranty phase economically viable. If the degradation rate stays the same, such modules will deliver more than 16%$_{absolute}$ or 15.5%$_{absolute}$ after another 10 or 20 years, respectively. The lower range of warranties given by various manufacturers is, in the example of the 20% PERC module, 16%$_{absolute}$ after 25 years.

For these reasons, better stabilizing efficiency has very positive economic and environmental consequences. An alternative route to stabilise efficiency could be provided by doping with a different Group III element (e.g. aluminium, gallium or indium), with the aim of improved lifetime stability. Aluminium doping is not likely to be viable due to the strong recombination activity of aluminium-oxygen complexes [14,15]. Indium doped silicon has been used to make passivated emitter and rear cell (PERC) devices which are reported to be stable under illumination [16,17]. Unfortunately indium's acceptor level is moderately deep relative to the valence band edge (E_v + 0.156 eV), and this means that at room temperature it is not fully ionized [18]. The un-ionized indium acts as a recombination centre [18, 19] and the variation in effective doping level with temperature may be problematic in cell optimisation.

Gallium is the most promising of the alternative Group III dopants, and has been demonstrated to be viable from an industrial perspective [20]. Lifetimes in gallium doped monocrystalline silicon wafers are reportedly stable under low-temperature illumination, regardless of ingot position and oxygen levels [21,22]. Gallium doped passivated emitter [21] and aluminium back surface field (Al-BSF) [22] monocrystalline cells are reported to give stable efficiencies which are similar to initial efficiencies of cells processed under the same conditions made from boron doped substrates. Although early work reported lifetime in gallium doped mc-Si was stable under illumination [23], recent work has shown that fired mc-Si PERC devices degrade but to a lesser extent than boron doped cells [24]. Fired gallium doped mc-Si lifetime samples are also found to experience LeTID-like behaviour, with the degradation being slower than in the boron case [25,26]. Compared to boron doped silicon, there are relatively few published fundamental studies of what determines the lifetime in gallium doped silicon, but the formation and dissociation of FeGa pairs is known to be an important issue where Fe is present [27–31]. Copper contaminants also induce LID in gallium doped wafers, but to a lesser extent than in boron doped wafers [32]. To the best of our knowledge, no studies have been published which determine whether monocrystalline gallium doped wafers and cells change with low-temperature processing (<400 °C).

This paper provides the results of experiments into the bulk lifetime behaviour of gallium doped monocrystalline silicon wafers and completed PERC devices made from gallium doped monocrystalline substrates ("Ga PERC"). We first briefly report results for as-grown wafer material, showing lifetimes can be influenced by low-temperature annealing and illumination due to dissociation of metastable defects. With the knowledge of how to control the influence of metastable defects, we then study commercially processed PERC devices, and compare our results to PERC devices produced with the same fabrication process using boron doped substrates ("B PERC") with the addition of a final stabilisation step. Using a proxy non-contact method based upon photoluminescence (PL) imaging to characterise the cell properties, we find that Ga PERC devices not annealed after fabrication are stable within 5%, but if annealed at 200 °C–300 °C they exhibit a noticeable level of degradation. Ga PERC devices without stabilisation show considerably better stability than the destabilised B PERC devices. Finally, we then strip processed cells at various stages of degradation to

link the cell level changes to changes in bulk lifetime in the substrate.

2. Experimental methods

Experiments were performed on commercial 15.6 cm × 15.6 cm PERC solar cells fabricated from either Ga and B doped (100)-orientation Czochralski silicon (Cz-Si) substrates, with an identical fabrication procedure on the same fabrication line. The cells were taken from a standard manufacturing line, processed in a standard way with no unusual processing steps. All cells were therefore fired after screen printing. The wafer resistivity and thickness range were 1.2–1.5 Ωcm and 140–150 μm, respectively. The B PERC devices were stabilised with the dark-current procedure described in the introduction, where the temperature is not measured nor controlled very precisely, but the procedure has been optimized with extensive field tests. In contrary, the Ga PERC cells were not exposed to any after-treatment. Experiments were also performed on 'as-received' 190 μm thick 156 mm diameter 1.7 Ωcm Ga doped (100)-orientation Cz-Si wafers, which were similar to those used in the Ga PERC devices. For control purposes, 360 μm thick 2 Ωcm phosphorus doped n-type float-zone silicon (FZ-Si) samples were used to monitor surface passivation stability under illumination, and n-type material was chosen as it is less susceptible to bulk lifetime instabilities due to metastable metal-acceptor pairs and boron-oxygen LID often found in p-type silicon.

In this study, it was sometimes necessary to strip the PERC devices back to their underlying substrate and to passivate the surfaces using either a room temperature passivation treatment or by aluminium oxide (Al$_2$O$_3$) deposited with atomic layer deposition (ALD). Temporary passivation schemes (see Ref. [33] for a review) can enable the lifetime to be measured without thermal processing which can otherwise modify the material under investigation, so where this is a requirement we use superacid-derived passivation [34–36]. For the as-received Ga doped samples, superacid-derived passivation was performed using bis(trifluoromethane)sulfonimide (TFSI) from Sigma-Aldrich (95% purity) in anhydrous hexane (Sigma-Aldrich, >95% purity) using a procedure described in detail in Ref. [35]. For the stripped PERC devices, a slightly modified superacid-derived passivation method was required due to the remaining effects of the metallisation on the surface, as follows:

(i) Dip in 1% HF for 1 min to remove the native oxide.
(ii) Immersion in a silver etch solution consisting of NH$_4$OH (30%) and H$_2$O$_2$ (30%) in the ratio 1:1 for 10 min at ~75 °C.
(iii) Immersion in ~50% HF for 5 min.
(iv) Standard clean 1 (SC 1) consisting of de-ionized (DI) H$_2$O (18.2 MΩ), NH$_4$OH (30%), H$_2$O$_2$ (30%) in the ratio 5:1:1 for 10 min at ~75 °C.
(v) Dip in 1% HF for 1 min.
(vi) Aqua regia metal etch consisting of HCl (37%) and HNO$_3$ (69.5%) mixed in the ratio 3:1. This was left to react for 15 min before adding the samples, which were etched for 15 min.
(vii) Dip in 1% HF for 1 min, followed by SC 1, followed by dip in 1% HF.
(viii) Standard clean 2 (SC 2) consisting of DI H$_2$O, HCl (37%), H$_2$O$_2$ (30%) in the ratio 5:1:1 for 10 min at ~75 °C.
(ix) Dip in 1% HF for 1 min.
(x) Etch in 25% tetramethylammonium hydroxide (TMAH) for 30 min at ~80 °C.
(xi) Dip in 1% HF for 1 min, followed by SC 2 and a DI H$_2$O rinse.
(xii) Soak in a mixture of 1% HF and 1% HCl diluted with DI H$_2$O for 10 min, then pull dry the samples from the solution ready for superacid treatment.
(xiii) Dip in TFSI-hexane mixture for ~60 s in a glovebox with an ambient relative humidity of ~25%.

ALD Al$_2$O$_3$ surface passivation was used when longer term stability was required. For this, the surface preparation procedure involved a dip

in HF (2%), immersion in a silver etch solution for 10 min (see step (ii) above), immersion in ~50% HF for 5 min, SC1 clean for 5 min, a dip in HF (2%), a TMAH etch at 80 °C for 10 min, a dip in HF (2%), an SC2 clean for 10 min, and a final HF dip (2%). Samples were pulled dry from the final HF dip (*i.e.* no rinsing) and were immediately transferred to a Veeco Fiji G2 ALD system where they were rapidly held under vacuum to prevent surface oxidation. Al_2O_3 was deposited at 200 °C using a plasma O_2 source and a trimethylaluminium precursor for 300 cycles to give films ~30 nm thick. The samples were then turned over and the same deposition conditions were used to deposit Al_2O_3 on the other surface. To activate the passivation, a post-deposition anneal in air was performed in a clean tube furnace at either 420 or 460 °C for 30 min.

Annealing other than for passivation activation was performed in one of two ways. As-received wafer samples were first subjected to a cleaning procedure, which including a rinse in DI water, a 2% HF dip (1 min), a SC 2 clean, a DI water rinse, followed by another 2% HF dip (1 min). They were then annealed in a clean tube furnace in air at 200–500 °C, followed by cleaning as part of the surface passivation procedure. PERC samples could not be cleaned due to the metallisation and were annealed in a standard box furnace in air at 200–300 °C.

Effective lifetime measurements of passivated samples were made by transient and generalised photoconductance methods using a Sinton WCT-120 lifetime tester which uses a Quantum Qflash X5d-R flash lamp with an infrared pass filter. This was calibrated using a recently introduced method [37]. To monitor the performance of processed cells after thermal and illumination treatments, a proxy method was developed using PL imaging. This was performed in a BT Imaging LIS-L1 system in which a 630 nm light emitting diode array is used to illuminate the samples. As illustrated in Fig. 1, the method involved selecting an approximate 2 cm × 2 cm region of interest (ROI) away from the edges of a 5 cm × 5 cm sample and recording the total number of PL counts after an 1 Sun exposure for 0.1–0.5 s. Care was taken to monitor the exact same region after each illumination step. The ROI was always scratch free and a significant region around the ROI was also ensured to be scratch free as lateral conduction could affect the PL signal. The advantage of this method is that it is contactless and so the sample does not get damaged as a consequence of a large number (up to ~50) of

measurements, which would be much more difficult to achieve with a contacted cell measurement considering today's fine-line screen printing of the 12 narrow busbars. A disadvantage is that the method provides only a relative measurement of performance of a given device sample, with comparisons between devices difficult because of differences caused by spatial variation in PL counts of the original 156 mm × 156 mm PERC device and varying levels of shading within the ROIs due to the metallisation.

Illumination experiments on as-received wafer samples were performed using the PL imaging system with a 1 Sun exposure applied for 10 s at room temperature. Light soaking experiments on PERC samples were conducted by placing samples on hotplates to maintain the sample temperature at 75 °C when illuminated with a halogen lamp. One Sun equivalent illumination was achieved by adjusting the lamp height until a power density of ~1000 Wm^{-2} was measured using an Amprobe Solar-100 m (see Ref. [38] for an accurate quantification of 'Sun equivalent').

3. Results & discussion

3.1. Lifetime instabilities in unprocessed Ga doped wafers

We first report lifetime results for samples extracted from as-received gallium doped Cz-Si wafers. These results, which are shown in Fig. 2, include the effect of low-temperature annealing on lifetime, and the stability data are important in establishing the consistency of the measurements used at the cell level later in the paper.

Fig. 2(a) shows the impact of low temperature annealing on the effective lifetime at an excess carrier density, Δn, of 10^{15} cm^{-3}. For these experiments, room temperature superacid-derived surface passivation was used, as other surface passivation processes such as ALD Al_2O_3 require elevated temperatures (for deposition and activation annealing) which will change the bulk lifetime under investigation as discussed in Ref. [33]. The surface recombination velocity (SRV) for superacid-derived passivation is higher than for our ALD Al_2O_3 passivation, and is typically around 1 cm/s [34,35]. The effective lifetimes in Fig. 2(a) are lower than they would be with our Al_2O_3 passivation, but it remains possible to distinguish changes in the bulk lifetime which occur only due to thermal effects. All lifetime measurements for Fig. 2(a) were made without intense illumination with sufficient time left after any annealing for any metastable recombination-active defects (*e.g.* FeGa pairs [29]) to have returned to their equilibrium state.

The squares in Fig. 2(a) denote lifetimes measured prior to annealing. The average as-received effective lifetime is 439 μs, with the lowest measurement being 423 μs and the highest 460 μs. Differences in lifetime relative to the mean are within ±5% and so can be assumed to be the same given the typical reproducibility of lifetime measurements [39] and the surface passivation scheme used [35]. The circles in Fig. 2(a) denote lifetimes after low-temperature annealing, and in all cases the lifetime has increased as a result of the thermal processing. A transition in lifetime occurs between 300 °C and about 380 °C, and this may be due to the annealing out of recombination-active defects, with the improvement being less pronounced at 500 °C. Lifetime instabilities at low processing temperatures have been found to occur in a range of silicon material types. For example, lifetime increases in *n*-type Cz-Si between 300 and 400 °C [40] have been linked to the annealing out of vacancy-oxygen related defects [41]. Studies on *p*-type and *n*-type float-zone silicon (FZ-Si) have also shown an increase in lifetime with annealing up to 320 °C and decrease in lifetime at 450 °C [42,43]. Thus, whilst lifetime changes occur in gallium doped Cz-Si at low temperatures, there is no evidence that this is due to the gallium and it seems more likely that it is related to reconfiguration of grown-in crystal defects as happens in materials grown with other dopants. Much stronger transitions around 350 °C have been specifically associated with gallium in electron irradiated Cz-Si [44], but the likely vacancy concentration in that material is much higher than in ours and in other materials used in the silicon photovoltaics industry, and so the effects are most likely
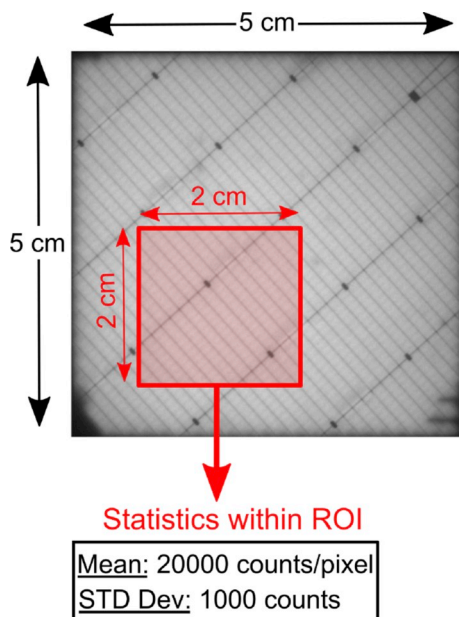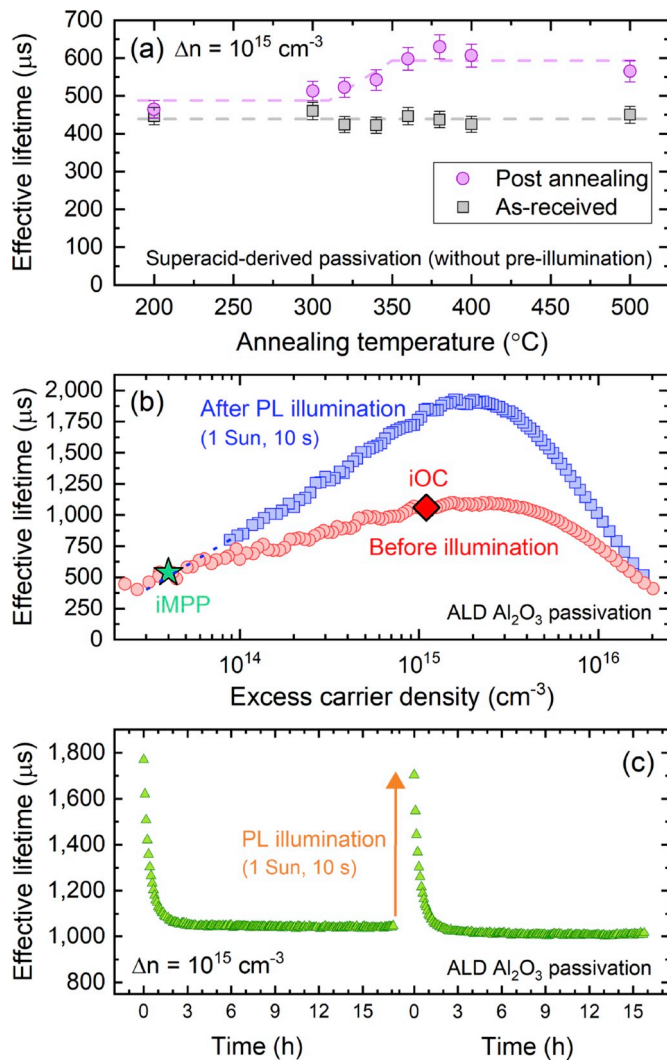

Fig. 1. A schematic of the PL proxy method used to study completed PERC devices in this work. A damage-free region of interest (ROI) is chosen away from the edges of a PERC cell sample. The mean number of counts from this region is recorded at all stages of light soaking. The example shown is a PL image of a sample from a Ga PERC device.

Fig. 2. Effective lifetime results for 1.7 Ωcm Ga doped Cz-Si substrates which had not been subjected to cell processing. (a) Lifetime results before and after annealing for 30 min at the low temperature plotted measured with room temperature superacid-derived passivation without pre-illumination (*i.e.* with FeGa pairs associated). (b) Typical injection-dependent lifetime results for Ga doped samples with ALD Al_2O_3 surface passivation with implied maximum power point (iMPP) and before illumination implied open circuit (iOC) conditions shown. The data shown are for a sample which has undergone a 30 min anneal at 400 °C to maximise lifetime, then a 30 min 460 °C activation anneal after ALD. (c) Effective lifetime versus time after illumination (1 Sun, 10 s) in the same ALD passivated sample as in (b). Illumination for (b) and (c) was performed in the PL imaging system at room temperature.

different.

Fig. 2(b) shows room temperature injection-dependent effective lifetime data for an ALD Al_2O_3 passivated Ga doped sample. The data are for a sample which had been pre-annealed at 400 °C (30 min) to maximise lifetime based on Fig. 2(a) results, but the subsequent Al_2O_3 activation anneal at 460 °C (30 min) probably overwrites this anyway. Importantly the effective lifetime is strongly affected by illumination, with the peak value increasing from 1100 μs to 1930 μs when 1 Sun is applied for 10 s. The implied maximum power point (iMPP) and implied open circuit (iOC) condition are indicated on Fig. 2(b) as if this wafer were a finished PERC device. These values were determined using Trina Solar's detailed numerical model for the cell type investigated in this paper. The annealing would only increase V_{oc} but not V_{mpp}, hence it would lower the fill factor and leave cell efficiency unaffected. Fig. 2(c) shows the kinetics of the lifetime change at $\Delta n = 10^{15}$ cm^{-3}. Illumination

increases the lifetime substantially and the lifetime decays back down to the pre-illuminated value over the period of a few hours. The effect can be cycled.

The lifetime changes which occur in Ga doped silicon upon illumination such as those in Fig. 2(b) and (c) are reasonably well understood in terms of the un-pairing and re-pairing of the FeGa pair [27–31]. Once dissociated by the illumination, the pairs re-form via room temperature diffusion of interstitial iron. The "after illumination" lifetime curve in Fig. 2(b) is therefore at least partly determined by recombination at dissociated Fe_i^+ and Ga$^-$, and the "before illumination" curve is partly determined by recombination at the FeGa pair. The characteristic cross-over in the lifetime curves for this situation is expected at around 3×10^{13} cm^{-3} at room temperature [29]. Whilst this relatively low injection level was not reliably achieved with our measurement set up with the high lifetimes after illumination, extrapolation of the curves from higher injection shown by the dotted line on Fig. 2(b) is consistent with this cross-over level.

The large range of possible lifetimes measured in the same sample in Fig. 2(b) and (c) highlights the need for a consistent methodology when studying Ga PERC devices. In the remainder of this paper, unless noted otherwise, the measurements are therefore reported after illumination with the FeGa pairs dissociated.

3.2. Light-induced degradation in commercially produced PERC devices

Fig. 3 plots the normalised PL intensity from our proxy method (Fig. 1) for B PERC and Ga PERC samples versus light soaking time at 1 Sun intensity and 75 °C. Note the vertical axes necessarily have different scales, as the magnitude of the effects observed in the B PERC is considerably larger than in the Ga PERC case. The four samples used for each dopant were cleaved from a single PERC device. To establish the impact of dark annealing on the LID characteristics, each cell sample was processed differently with one subjected to no anneal, and the others subjected to anneals at 200 °C, 250 °C or 300 °C for 30 min in air in a box furnace.

Firstly, it is important to note that the B PERC devices have undergone a dark-current stabilisation step in order to mitigate boron-oxygen LID [45,46]. In contrast, the Ga PERC devices have not undergone any final stabilisation process, as literature results have indicated that gallium doped silicon is immune to LID [21,22]. In order to establish if Ga PERC devices are indeed immune to LID, we have performed a side-by-side comparison between B PERC and Ga PERC devices after light soaking, whereby the primary difference is the dopant in the base silicon material.

For the B PERC devices shown in Fig. 3(a), it is evident from the green triangles that the stabilisation process has indeed mitigated the onset of degradation (both boron-oxygen and LeTID) for the sample which has not undergone a dark anneal in our laboratory. Interestingly, we find the normalised PL intensity exceeds unity after 10 h of illumination. It is difficult to ascertain the source of this increase definitively, however Sperber et al. have attributed a similar increase to improved surface passivation [47]. Whether it be an improvement in surface or bulk lifetime, an increase in performance under light soaking is a pleasing observation, and reflects the positive steps made over the past decades to improve and stabilise p-type silicon. In contrast, when the stabilised B PERC samples were dark annealed prior to light soaking, we observe a degradation in PL signal followed by a recovery, and thus reminiscent of a LeTID-like signature, *i.e.* a reduction in PL intensity followed by a complete recovery [4–10]. For the 250 °C and 300 °C samples, the recovery quickly transitioned into an overall improvement in performance relative to the first data point in the respective sample, as evidenced by the normalised PL intensity exceeding unity. With our proxy technique it is not possible to ascertain whether there is an absolute improvement relative to the sample which had not been dark annealed however. Notably, the low-temperature dark anneal has destabilised the previously stabilised B PERC devices, and the extent of
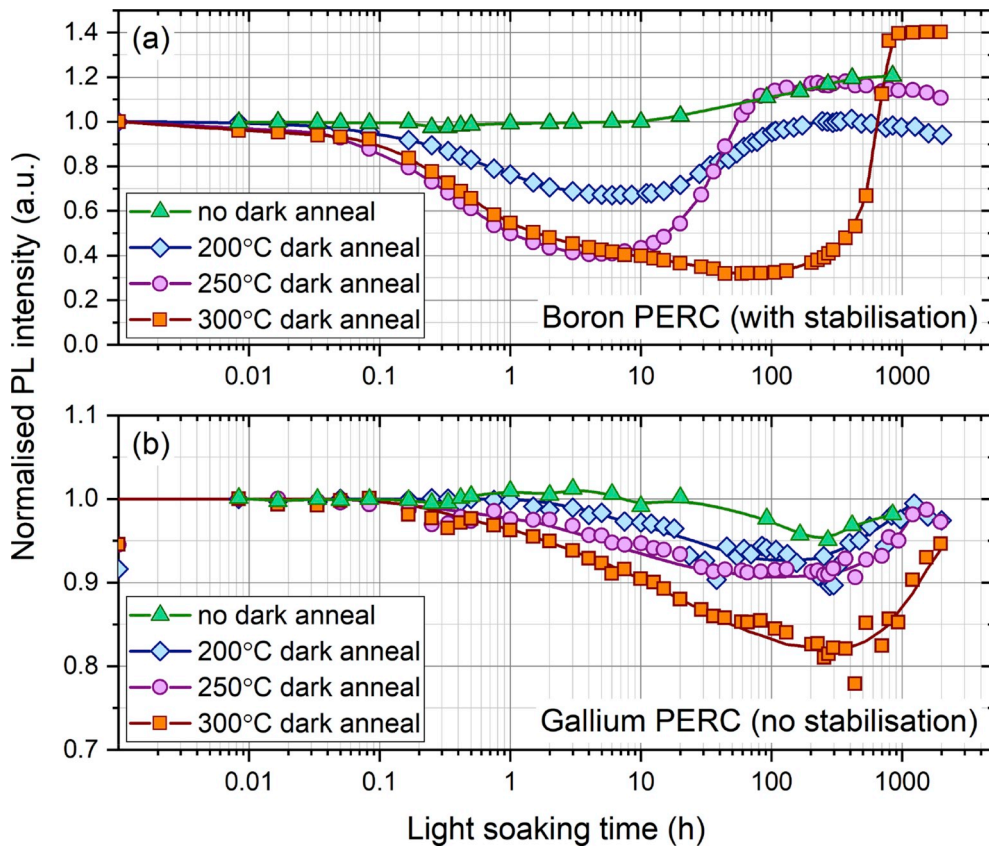
Fig. 3. Normalised PL intensity from the proxy method versus light soaking time at 1 Sun and 75 °C for PERC devices processed from (a) boron doped and (b) gallium doped substrates, with a stabilisation process having been performed on the former and not the latter. Note the different vertical scales, as the degradation is much less severe in the Ga PERC than in the B PERC case. The triangles are for cells which had not been subjected to a dark anneal prior to light soaking. The diamonds, circles and squares after for cells having had a 200 °C, 250 °C and 300 °C 30 min dark anneal prior to light soaking, respectively. Solid lines are guides to the eye. For a given device sample, normalisation was performed relative to the first point in the B PERC case, and relative to the second point in the Ga PERC case due to the metastable defect activity discussed in the text.

the degradation increases with increasing dark annealing temperature. The source of destabilisation is unclear at this time. Importantly, Fig. 3 (a) helps validate our PL proxy method, as the results resemble trends typically observed in lifetime samples which undergo LeTID [4–10].

Turning our attention to the Ga PERC results in Fig. 3(b), a clear observation is that all samples subjected to light soaking do degrade to some degree, although it is noted that these samples have not been stabilised in the same way as the B PERC devices. The extent of the degradation for Ga PERC is much reduced compared to the corresponding dark annealed B PERC devices. The reduced normalised PL value for the very first measurements in Fig. 3(b) suggests that associated FeGa pairs in the Ga PERC devices reduce the bulk lifetime, as demonstrated in Fig. 2(b) and (c) at the substrate level. However, for subsequent measurements, the prolonged light soaking results in a higher proportion of the FeGa pairs being in the dissociated state, and thus their impact on the bulk lifetime is reduced under the conditions used.

As in the case for the B PERC samples, subjecting the Ga PERC samples to a 30 min dark anneal does induce a LeTID-like degradation curve when subject to light soaking, and this becomes more pronounced with higher annealing temperatures. Again, it is unclear why a dark anneal would trigger such a LeTID curve, or why a higher annealing temperature would induce a stronger degradation effect, however it is evident that Ga PERC devices are not completely immune to LeTID. Furthermore, the similarity in degradation curves observed for both Ga and B PERC devices (*i.e.* degradation and recovery), may indicate the source of the degradation originates from a process induced defect, *e.g.* SiN_x:H dielectrics and firing [9,48], rather than a dopant related defect as supported by the work of Chen et al. [49].

In the context of Ga PERC devices, the most important data set is that relating to the un-annealed PERC sample (green triangles) in Fig. 3(b). In contrast to the stabilised B PERC device (no anneal) in Fig. 3(a), the Ga cell is not completely stable, and we do see a slight degradation after

~20 h of illumination, which is expected to recover by 1000 h. Providing the degradation does indeed not continue, it is still evident that the Ga PERC device is advantageous over B PERC, as it does not require an additional stabilisation process, and as such, could add potential cost savings to the manufacturing of high efficiency PERC devices and to PV utilities. Although a dark anneal was required to invoke a substantial level of degradation in the Ga PERC devices, it does mean that future processing sequences (*e.g.* production of passivated contact structures) may trigger the same LeTID signature during cell operation. This issue will not be as big an issue for manufacturers as permanent LID, but it is a factor which should be considered in the development of solar cell structures involving gallium doped substrates.

3.3. Correlating PL proxy degradation results with bulk lifetime changes in PERC devices

The results obtained using the PL proxy method in Fig. 3 show a clear degradation in the Ga PERC devices, but they do not prove that the degradation is caused by a reduction in bulk lifetime, as is known to be the case for boron doped lifetime samples [7,50]. Other effects could be occurring, such as a deterioration in the surface passivation. We have therefore performed an experiment to demonstrate that bulk lifetime degradation is occurring in the Ga PERC case, and the results are shown in Fig. 4.

The experiment used two 5 cm × 5 cm samples cleaved from the same 15.6 cm × 15.6 cm PERC device. Both samples were dark annealed at 300 °C for 30 min to trigger the strongest case of LeTID-like behaviour shown by the orange squares in Fig. 3(b). The samples were then characterised by the PL imaging proxy method to determine their pre-LID values, and to ensure the samples were similar. One sample was stored in the dark, while the other was subjected to light soaking at 1 Sun and 75 °C for ~100 h, which according to Fig. 3(b) will give rise to substantial degradation. Both samples were re-characterised using the
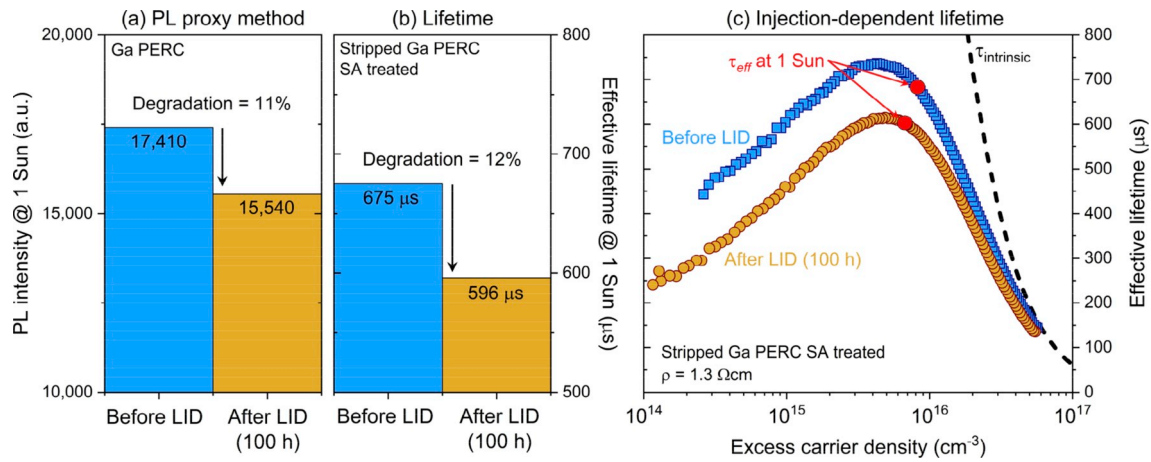
Fig. 4. A validation of the PL proxy method for Ga PERC devices subjected to 300 °C dark annealing. (a) The PL proxy intensity results for a Ga PERC device before and after 100 h of LID (1 Sun, 75 °C). (b) Effective lifetime in stripped Ga PERC devices with superacid-derived passivation ("SA treated") before and after 100 h of LID (1 Sun, 75 °C). (c) Injection-dependent effective lifetime measurements of the stripped Ga PERC device with superacid-derived passivation. The intrinsic lifetime limit of Richter et al. [51] is also plotted.

PL imaging proxy method. Fig. 4(a) shows the results of the tests, with an 11% reduction in PL observed. The metallisation and diffusions were then stripped away from the surfaces of the two samples, and the effective lifetimes were measured with the room temperature superacid-derived passivation treatment [34–36]. The effective lifetime data are shown in Fig. 4(b) and show practically the same (12%) reduction between the two samples at an excess carrier density corresponding to 1 Sun illumination as determined using the reference cell in the lifetime tester. From the results in Fig. 4, it is evident that bulk lifetime degradation is causing the PERC degradation, and the similar quantitative reductions in PL or effective lifetime suggest it is the dominant effect.

Fig. 4(c) shows the injection-dependent lifetime and its value at 1 Sun of these passivated samples with a comparison to the intrinsic lifetime limit of Richter et al. [51].

3.4. Lifetime stability in pre-stripped gallium PERC devices

Our final set of experiments aims to understand the degradation of bulk lifetime in gallium doped silicon wafers which have been processed into PERC devices then stripped prior to illumination. Our experimental design is illustrated schematically in Fig. 5, and this methodology enables us to report effective lifetime values rather than PL proxy data.
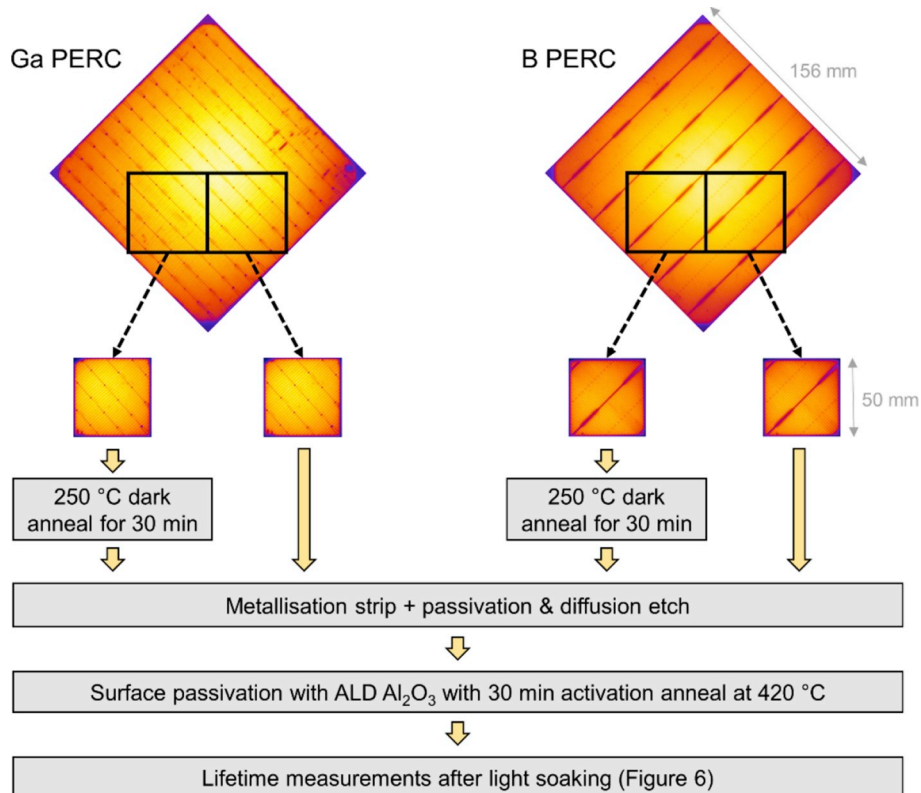
Fig. 5. Schematic to show the design of experiments to test lifetime stability in PERC devices. Two samples are extracted from Ga PERC device (without a stabilisation treatment) and a B PERC device (with a stabilisation treatment) and are processed as indicated above. The results from these experiments are shown in Fig. 6.
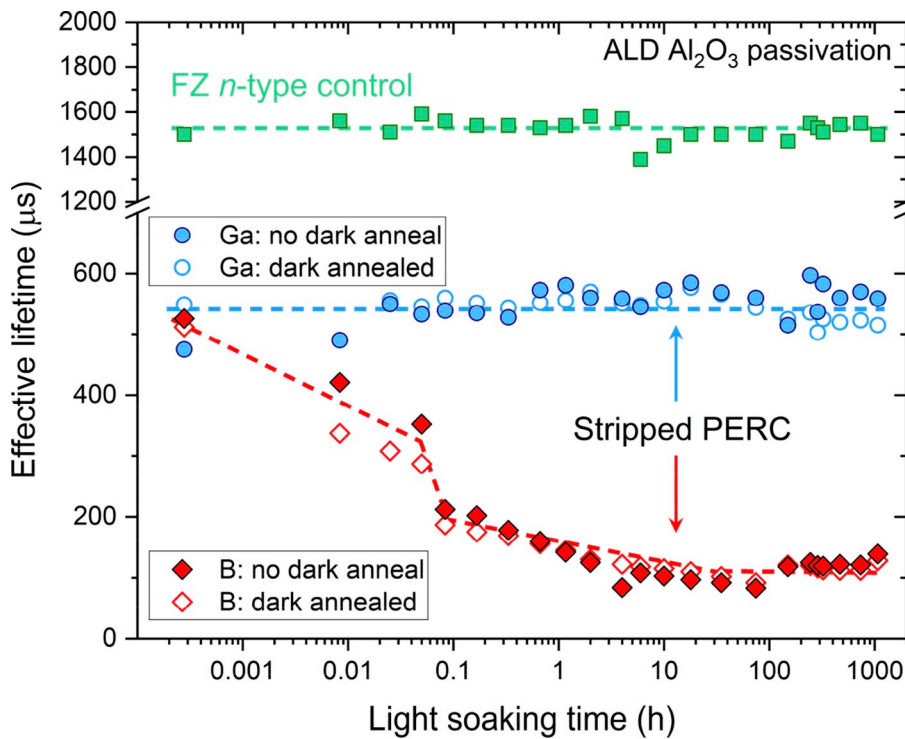
Fig. 6. Effective lifetime versus light soaking time at 1 Sun and 75 °C for samples processed in accordance with Fig. 5. Samples from Ga and B PERC devices had had their metallisation, dielectric coatings and diffusions stripped prior to passivation by ALD Al$_2$O$_3$ (activated at 420 °C). 'Dark annealed' corresponds to the PERC devices subjected to a 250 °C dark anneal for 30 min prior to being stripped. To exclude possible surface passivation degradation effects, a FZ 2 Ω-cm *n*-type control sample was used to monitor the passivation stability. The dashed lines are guides to the eye.

Stable surface passivation is needed for these experiments, and ALD Al$_2$O$_3$ deposited at 200 °C and activated by a 420 °C anneal was used. The lifetime results are shown in Fig. 6.

Importantly, it is first noted that the surface passivation is stable under illumination, evidenced by the FZ *n*-type control data in Fig. 6, and thus any degradation observed can be attributed to a reduction in the bulk lifetime. Secondly, the 250 °C dark anneal prior to stripping the PERC devices has made no difference to the light soaking trends, suggesting the ALD process (most likely the 420 °C activation anneal) has changed the bulk lifetime characteristics, and therefore annihilated any prior defect the 250 °C dark anneal activates, as observed in Fig. 3.

In the case of the stripped B PERC devices (red diamonds), the degradation characteristics have completely changed compared to those shown for the unstripped B PERC device in Fig. 3. The trend shown in Fig. 6 now closely resembles that of the boron-oxygen defect, suggesting that the effects of the stabilisation process has been undone. That is, there is an initial fast degradation, followed by a much slower one whereby the bulk lifetime does not recover unless subject to a dark anneal [3,52]. For the stripped Ga PERC devices (blue circles), the lifetime remains stable, and no degradation can be observed, consistent with previous reports on gallium doped silicon [21,22]. Therefore in contrast to Fig. 3, the same trends could not be observed, indicating the ALD process has changed the bulk lifetime characteristics and its corresponding LID signature. Finally, it is noted that the constant lifetime in ALD Al$_2$O$_3$ passivated stripped Ga PERC material in Fig. 6 provides further evidence that the passivation on *p*-type material is stable under illumination, which needs to be demonstrated because it has been suggested that Fermi level position might affect the surface behaviour [47].

The results shown in Fig. 6 demonstrate that extreme care must be taken when using dielectric passivation structures to analyse the bulk lifetime of stripped PERC devices. Low temperature annealing (which is required to activate ALD Al$_2$O$_3$ surface passivation), can significantly change the bulk lifetime characteristics and thus its susceptibility (or resilience) to LID.

4. Conclusions

We examined the degradation trends of B and Ga monocrystalline PERC devices when exposed to 1 Sun illumination at 75 °C for >1000 h. In the "as-produced" state which included a stabilisation step, the B PERC device indeed remained stable, or underwent a slight relative improvement. In the case of the as-produced Ga PERC device (without a stabilisation step), we observed a slight degradation (∼5%) in performance which is expected to recover by 1000 h. When the B and Ga PERC devices were subjected to a dark anneal at 200, 250 or 300 °C prior to light soaking, we observed significant changes in the LID characteristics of the cells. All previously stabilised B PERC devices underwent a fast degradation followed by a complete recovery, characteristic of LeTID, indicating the low-temperature dark anneal has undone the effects of stabilisation. A similar trend was also observed for Ga PERC devices which had not been subjected to a stabilisation treatment, showing LeTID can also occur in Ga doped silicon. After stripping degraded Ga PERC devices, it was determined that the cause of this degradation is a deterioration in the bulk lifetime, consistent with that found previously for boron doped samples. When the Ga and B PERC cells were stripped and passivated with ALD Al$_2$O$_3$, we observed a complete change in the degradation characteristics, *i.e.* no degradation for Ga, and boron-oxygen-like degradation for B. This indicates that dielectric passivation is not adequate to diagnose bulk lifetime degradation causes in stripped PERC devices.

It is evident that Ga PERC is advantageous over B PERC, as it does not require an additional stabilisation process, and, as such, could add potential cost savings to the manufacturing of high efficiency PERC devices and to PV utilities. However, manufacturers looking to substitute B PERC with Ga PERC need to be aware that any future fabrication processes (*e.g.* passivated contact structures) could make Ga PERC solar cells susceptible to degradation, and thus care must be taken.

Author contribution

Nicholas E. Grant: Conceptualization, Methodology, Investigation, Writing - Original Draft, Visualization, Supervision, Funding

acquisition. **Jennifer R. Scowcroft**: Investigation. **Alex I. Pointon**: Investigation. **Mohammad Al-Amin**: Investigation. **Pietro P. Altermatt**: Resources, Writing - Review & Editing. **John D. Murphy**: Conceptualization, Resources, Data Curation, Writing - Original Draft, Visualization, Supervision, Project administration, Funding acquisition.

Access to data statement

Data published in this article can be freely downloaded from https://wrap.warwick.ac.uk/129659/.

Declaration of competing interest

The authors declare that they have no known competing financial interests or personal relationships that could have appeared to influence the work reported in this paper.

Acknowledgements

References

[1] H. Fischer, W. Pschunder, Investigation of photon and thermal induced changes in silicon solar cells, 10th IEEE Photovoltaic Specialists Conference (Palo Alto, CA, USA, 1973), p. 404.
[2] J. Lindroos, H. Savin, Review of light-induced degradation in crystalline silicon solar cells, Sol. Energy Mater. Sol. Cells 147 (2016) 115–126, https://doi.org/10.1016/j.solmat.2015.11.047.
[3] T. Niewelt, J. Schön, W. Warta, S.W. Glunz, M.C. Schubert, Degradation of crystalline silicon due to boron–oxygen defects, IEEE J. Photovolt. 7 (2017) 383–398, https://doi.org/10.1109/JPHOTOV.2016.2614119.
[4] F. Kersten, P. Engelhart, H.-C. Ploigt, A. Stekolnikov, T. Lindner, F. Stenzel, M. Bartzsch, A. Szpeth, K. Petter, J. Heitmann, J.W. Müller, Degradation of multicrystalline silicon solar cells and modules after illumination at elevated temperature, Sol. Energy Mater. Sol. Cells 142 (2015) 83–86, https://doi.org/10.1016/j.solmat.2015.06.015.
[5] M.A. Jensen, A.E. Morishige, J. Hofstetter, D.B. Needleman, T. Buonassisi, Evolution of LeTID defects in *p*-type multicrystalline silicon during degradation and regeneration, IEEE J. Photovolt. 7 (2017) 980–987, https://doi.org/10.1109/JPHOTOV.2017.2695496.
[6] D. Bredemeier, D.C. Walter, J. Schmidt, Possible candidates for impurities in mc-Si wafers responsible for light-induced lifetime degradation and regeneration, Solar RRL 2 (2018), 1700159, https://doi.org/10.1002/solr.201700159.
[7] T. Niewelt, M. Selinger, N.E. Grant, W.M. Kwapil, J.D. Murphy, M.C. Schubert, Light-induced activation and deactivation of bulk defects in boron-doped float-zone silicon, J. Appl. Phys. 121 (2017), 185702, https://doi.org/10.1063/1.4983024.
[8] D. Sperber, A. Herguth, G. Hahn, A 3-state defect model for light-induced degradation in boron-doped float-zone silicon, Phys. Status Solidi Rapid Res. Lett. 11 (2017), 1600408, https://doi.org/10.1002/pssr.201600408.
[9] D. Chen, M. Kim, B.V. Stefani, B.J. Hallam, M.D. Abbott, C.E. Chan, R. Chen, D.N. R. Payne, N. Nampalli, A. Ciesla, T.H. Fung, K. Kim, S.R. Wenham, Evidence of an identical firing-activated carrier-induced defect in monocrystalline and multicrystalline silicon, Sol. Energy Mater. Sol. Cells 172 (2017) 293–300, https://doi.org/10.1016/j.solmat.2017.08.003.
[10] D. Sperber, A. Schwarz, A. Herguth, G. Hahn, Bulk and surface-related degradation in lifetime samples made of Czochralski silicon passivated by plasma-enhanced chemical vapor deposited layer stacks, Phys. Status Solidi A 215 (2018), 1800741, https://doi.org/10.1002/pssa.201800741.
[11] T. Niewelt, F. Schindler, W. Kwapil, R. Eberle, J. Schön, M.C. Schubert, Understanding the light-induced degradation at elevated temperatures: similarities between multicrystalline and floatzone p-type silicon, Prog. Photovolt. Res. Appl. 26 (2018) 533–542, https://doi.org/10.1002/pip.2954.
[12] A. Inglese, J. Lindroos, H. Vahlman, H. Savin, Recombination activity of light-activated copper defects in p-type silicon studied by injection- and temperature-dependent lifetime spectroscopy, J. Appl. Phys. 120 (2016), 125703, https://doi.org/10.1063/1.4963121.
[13] S. Wilking, C. Beckh, S. Ebert, A. Herguth, G. Hahn, Influence of bound hydrogen states on BO-regeneration kinetics and consequences for high-speed regeneration processes, Sol. Energy Mater. Sol. Cells 131 (2014) 2–8, https://doi.org/10.1016/j.solmat.2014.06.027.
[14] J. Schmidt, Temperature- and injection-dependent lifetime spectroscopy for the characterization of defect centers in semiconductors, Appl. Phys. Lett. 82 (2003) 2178–2180, https://doi.org/10.1063/1.1563830.
[15] P. Rosenits, T. Roth, S.W. Glunz, S. Beljakowa, Determining the defect parameters of the deep aluminum-related defect center in silicon, Appl. Phys. Lett. 91 (2007), 122109, https://doi.org/10.1063/1.2789378.
[16] E. Cho, Y.-W. Ok, A.D. Upadhyaya, M.J. Binns, J. Appel, J. Guo, A. Rohatgi, P-type indium-doped passivated emitter rear solar cells (PERC) on Czochralski silicon without light-induced degradation, IEEE J. Photovolt. 6 (2016) 795–800, https://doi.org/10.1109/JPHOTOV.2016.2547578.
[17] N. Balaji, V. Shanmugam, S. Raj, J.M.Y. Ali, M.L.O. Aguilar, I.J. Garcia, J. Rodriguez, A. Aberle, S. Duttagupta, Impact of light soaking on p-type boron- and indium-doped passivated emitter and rear solar cells on Czochralski-grown silicon, Solar RRL 3 (2019), 1900027, https://doi.org/10.1002/solr.201900027.
[18] J.D. Murphy, A.I. Pointon, N.E. Grant, V.A. Shah, M. Myronov, V.V. Voronkov, R. J. Falster, Minority carrier lifetime in indium doped silicon for photovoltaics, Prog. Photovolt. Res. Appl. 27 (2019) 844–855, https://doi.org/10.1002/pip.3172.
[19] M.J. Binns, J. Appel, J. Guo, H. Hieslmair, J. Chen, T.N. Swaminathan, E.A. Good, Indium-doped mono-crystalline silicon substrates exhibiting negligible lifetime degradation following light soaking, in: Proceedings of the 42nd IEEE Photovoltaic Conference, 2015, https://doi.org/10.1109/PVSC.2015.7355617.
[20] G. Crabtree, T.L. Jester, C. Fredric, J. Nickerson, V. Meemongkolkiat, A. Rohatgi, Production viability of gallium doped mono-crystalline solar cells, in: *31st IEEE Photovoltaic Specialists Conference* (Lake Buena Vista, FL, USA, 2005, p. 935, https://doi.org/10.1109/PVSC.2005.1488285.
[21] S.W. Glunz, S. Rein, J. Knobloch, W. Wettling, T. Abe, Comparison of boron- and gallium-doped p-type Czochralski silicon for photovoltaic application, Prog. Photovolt. Res. Appl. 7 (1999) 463–469, https://doi.org/10.1002/(SICI)1099-159X(199911/12)7:6%3C463::AID-PIP293%3E3.0.CO;2-H.
[22] V. Meemongkolkiat, K. Nakayashiki, A. Rohatgi, G. Crabtree, J. Nickerson, T. L. Jester, Resistivity and lifetime variation along commercially grown Ga- and B-Doped Czochralski Si ingots and its effect on light-induced degradation and performance of solar cells, Prog. Photovolt. Res. Appl. 14 (2006) 125–134, https://doi.org/10.1002/pip.659.
[23] M. Dhamrin, H. Hashigami, T. Saitoh, Elimination of light-induced degradation with gallium-doped multicrystalline silicon wafers, Prog. Photovolt. Res. Appl. 11 (2003) 231–236, https://doi.org/10.1002/pip.482.
[24] S. Zhang, J. Peng, H. Qian, H. Shen, Q. Wei, W. Lian, Z. Ni, J. Jie, X. Zhang, L. Xie, The impact of thermal treatment on light-induced degradation of multicrystalline silicon PERC solar cell, Energies 12 (2019) 416, https://doi.org/10.3390/en12030416.
[25] J. Fritz, A. Zuschlag, D. Skorka, A. Schmid, G. Hahn, Impact of temperature and doping on LeTID and regeneration in mc-Si, in: 33rd European Photovoltaic Solar Energy Conference and Exhibition (Amsterdam, The Netherlands), 2017, p. 569, https://doi.org/10.4229/EUPVSEC20172017-2AV.1.40.
[26] J.M. Fritz, A. Zuschlag, D. Skorka, A. Schmid, G. Hahn, Temperature dependent degradation and regeneration of differently doped mc-Si materials, Energy Procedia 124 (2017) 718–725, https://doi.org/10.1016/j.egypro.2017.09.085.
[27] J. Schmidt, D. Macdonald, Recombination activity of iron-gallium and iron-indium pairs in silicon, J. Appl. Phys. 97 (2005), 113712, https://doi.org/10.1063/1.1929096.
[28] Y. Yoon, Y. Yan, N.P. Ostrom, J. Kim, G. Rozgonyi, Deep level transient spectroscopy and minority carrier lifetime study on Ga-doped continuous Czochralski silicon, Appl. Phys. Lett. 101 (2012), 222107, https://doi.org/10.1063/1.4766337.
[29] T.U. Nærland, S. Bernardini, H. Haug, S. Grini, L. Vines, N. Stoddard, M. Bertoni, On the recombination centers of iron-gallium pairs in Ga-doped silicon, J. Appl. Phys. 122 (2017), 085703, https://doi.org/10.1063/1.5000358.
[30] R. Post, T. Niewelt, J. Schön, F. Schindler, M.C. Schubert, Imaging interstitial iron concentrations in gallium-doped silicon wafers, Phys. Status Solidi A 216 (2019), 1800655, https://doi.org/10.1002/pssa.201800655.
[31] R. Post, T. Niewelt, W. Yang, D. Macdonald, W. Kwapil, M.C. Schubert, Re-evaluation of the SRH-parameters for the FeGa defect, in: AIP Conference Proceedings, vol. 2147, 2019, p. 020012, https://doi.org/10.1063/1.5123817.
[32] J. Lindroos, M. Yli-Koski, A. Haarahiltunen, M.C. Schubert, H. Savin, Light-induced degradation in copper-contaminated gallium-doped silicon, Phys. Status Solidi Rapid Res. Lett. 7 (2013) 262–264, https://doi.org/10.1002/pssr.201307011.
[33] N.E. Grant, J.D. Murphy, Temporary surface passivation for characterisation of bulk defects in silicon: a review, Phys. Status Solidi Rapid Res. Lett. 11 (2017), 1700243, https://doi.org/10.1002/pssr.201700243.
[34] N.E. Grant, T. Niewelt, N.R. Wilson, E.C. Wheeler-Jones, J. Bullock, M. Al-Amin, M. C. Schubert, A.C. van Veen, A. Javey, J.D. Murphy, Superacid-treated silicon surfaces: extending the limit of carrier lifetime for photovoltaic applications, IEEE J. Photovolt. 7 (2017) 1574–1583, https://doi.org/10.1109/JPHOTOV.2017.2751511.
[35] A.I. Pointon, N.E. Grant, E.C. Wheeler-Jones, P.P. Altermatt, J.D. Murphy, Superacid-derived surface passivation for measurement of ultra-long lifetimes in silicon photovoltaic materials, Sol. Energy Mater. Sol. Cells 183 (2018) 164–172, https://doi.org/10.1016/j.solmat.2018.03.028.
[36] A.I. Pointon, N.E. Grant, R.S. Bonilla, E.C. Wheeler-Jones, M. Walker, P. R. Wilshaw, C.E.J. Dancer, J.D. Murphy, Exceptional surface passivation arising from bis(trifluoromethanesulfonyl)-based solutions, ACS Appl. Electron. Mater. 1 (2019) 1322–1329, https://doi.org/10.1021/acsaelm.9b00251.
[37] L.E. Black, D.H. Macdonald, Accounting for the Dependence of Coil Sensitivity on Sample Thickness and Lift-Off in Inductively Coupled Photoconductance Measurements, IEEE J. Photovolt. 9 (2019) 1563–1574, https://doi.org/10.1109/JPHOTOV.2019.2942484.

[38] A. Herguth, On the meaning(fullness) of the intensity unit 'suns' in light induced degradation experiments, Energy Procedia 124 (2017) 53–59, https://doi.org/10.1016/j.egypro.2017.09.339.

[39] A.L. Blum, J.S. Swirhun, R.A. Sinton, F. Yan, S. Herasimenka, T. Roth, K. Lauer, J. Haunschild, B. Lim, K. Bothe, Z. Hameiri, B. Seipel, R. Xiong, M. Dhamrin, J. D. Murphy, Inter-laboratory study of eddy-current measurement of excess-carrier recombination lifetime, IEEE J. Photovolt. 4 (2014) 525–531, https://doi.org/10.1109/JPHOTOV.2013.2284375.

[40] F.E. Rougieux, N.E. Grant, D. Macdonald, Thermal deactivation of lifetime limiting grown-in point defects in n-type Czochralski silicon wafers, Phys. Status Solidi Rapid Res. Lett. 7 (2013) 616–618, https://doi.org/10.1002/pssr.201308053.

[41] G.D. Watkins, Intrinsic defects in silicon, Mater. Sci. Semicond. Process. 3 (2000) 227–235, https://doi.org/10.1016/S1369-8001(00)00037-8.

[42] N.E. Grant, F.E. Rougieux, D. Macdonald, J. Bullock, Y. Wan, Grown-in defects limiting the bulk lifetime of p-type float-zone silicon wafers, J. Appl. Phys. 117 (2015), 055711, https://doi.org/10.1063/1.4907804.

[43] N.E. Grant, V.P. Markevich, J. Mullins, A.R. Peaker, F. Rougieux, D. Macdonald, Thermal activation and deactivation of grown-in defects limiting the lifetime of float-zone silicon, Phys. Status Solidi Rapid Res. Lett. 10 (2016) 443–447, https://doi.org/10.1002/pssr.201600080.

[44] A. Khan, M. Yamaguchi, Y. Ohshita, N. Dharmarasu, K. Araki, T. Abe, H. Itoh, T. Ohshima, M. Imaizumi, S. Matsuda, Role of the impurities in production rates of radiation-induced defects in silicon materials and solar cells, J. Appl. Phys. 90 (2001) 1170–1178, https://doi.org/10.1063/1.1384855.

[45] B.J. Hallam, P.G. Hamer, S.R. Wenham, M.D. Abbott, A. Sugianto, A.M. Wenham, C.E. Chan, G. Xu, J. Kraiem, J. Degoulange, R. Einhaus, Advanced bulk defect passivation for silicon solar cells, IEEE J. Photovolt. 4 (2014) 88–95, https://doi.org/10.1109/JPHOTOV.2013.2281732.

[46] C.E. Chan, D.N.R. Payne, B.J. Hallam, M.D. Abbott, T.H. Fung, A.M. Wenham, B. S. Tjahjono, S.R. Wenham, Rapid stabilization of high-performance multicrystalline P-type silicon PERC cells, IEEE J. Photovolt. 6 (2016) 1473–1479, https://doi.org/10.1109/JPHOTOV.2016.2606704.

[47] D. Sperber, A. Graf, D. Skorka, A. Herguth, G. Hahn, Degradation of surface passivation on crystalline silicon and its impact on light-induced degradation experiments, IEEE J. Photovolt. 7 (2017) 1627–1634, https://doi.org/10.1109/JPHOTOV.2017.2755072.

[48] D. Bredemeier, D.C. Walter, R. Heller, J. Schmidt, Impact of hydrogen-rich silicon nitride material properties on light-induced lifetime degradation in multicrystalline silicon, Phys. Status Solidi Rapid Res. Lett. 13 (2019), 1900201, https://doi.org/10.1002/pssr.201900201.

[49] D. Chen, P.G. Hamer, M. Kim, T.H. Fung, G. Bourret-Sicotte, S. Liu, C.E. Chan, A. Ciesla, R. Chen, M.D. Abbott, B.J. Hallam, S.R. Wenham, Hydrogen induced degradation: a possible mechanism for light- and elevated temperature- induced degradation in n-type silicon, Sol. Energy Mater. Sol. Cells 185 (2018) 174–182, https://doi.org/10.1016/j.solmat.2018.05.034.

[50] D. Sperber, A. Heilemann, A. Herguth, G. Hahn, Temperature and light-induced changes in bulk and passivation quality of boron-doped float-zone silicon coated with SiN$_x$:H, IEEE J. Photovolt. 7 (2017) 463–470, https://doi.org/10.1109/JPHOTOV.2017.2649601.

[51] A. Richter, S.W. Glunz, F. Werner, J. Schmidt, A. Cuevas, Improved quantitative description of Auger recombination in crystalline silicon, Phys. Rev. B 86 (2012), 165202, https://doi.org/10.1103/PhysRevB.86.165202.

[52] J. Schmidt, K. Bothe, Structure and transformation of the metastable boron- and oxygen-related defect center in crystalline silicon, Phys. Rev. B 69 (2004), 024107, https://doi.org/10.1103/PhysRevB.69.024107.